

Electromagnetically Coupled Semi-Circular Patch Antenna with Tapered Slotted Ground for V band, W Band and M Band Applications

Tapan Nahar¹, Sanyog Rawat^{*2}

Abstract – An electromagnetically linked semi-circular antenna with tapered slotted ground for broadband mm-wave applications is proposed in this communication. The presented antenna's bandwidth is increased by employing parasitically linked semi-circular patches with closed dimensions and a tapered slotted ground plane. At 60.4 GHz, the designed antenna has 70.83 % impedance bandwidth and produces less than 10% reflected power from 58.4 GHz to 100 GHz. At resonant frequency, the reflection coefficient is around -60 dB, and at most operating frequencies, it is less than -15 dB. Maximum gain is around 5.23 dB, with less than 1 dB of gain fluctuation in 75 % of the operating band and 2 dB variations in the whole operating band. Electromagnetic simulation tool Computer simulation technology microwave studio (CST Microwave Studio) is used for simulation. The proposed antenna has a small footprint of 3*3.5*0.4 mm³ and is built on a Rogers RO 3006 substrate with dielectric constant and loss tangent values of 6.5 and 0.002, respectively.

Keywords – mm-wave antenna, Tapered slot antenna, Parasitically coupled antenna, W-band antenna, V-band antenna.

I. INTRODUCTION

Higher frequencies can be used to evolve communications infrastructure to handle an increase in the number of users and the amount of data consumed by each user. To meet this requirement, next-generation communication systems will use V and W band frequencies (40-115) GHz. While terrestrial V and W band frequency linkages exist for short-distance communication, these bands have not been exploited for satellite communications (SATCOM). The strategic SATCOM application benefits from the utilization of these frequencies in numerous ways. Because of the small beam-width potential, detection and interception are unlikely. Since no commercial businesses currently use this band for SATCOM, huge sections of spectrum are available for this use. Ionospheric effects are less of an issue for higher frequency broadcasts. A satellite payload with a shorter antenna and device elements would occupy less space [1-12]. Various antennas [4-13] are reported for W-band and V-band communication in literature.

A parasitically coupled mm-wave patch antenna has been presented in [4] for 60 GHz applications. A slot is designed at

the partial ground plane below the feed line and patch junction, and the antenna is built on an LTCC substrate. Parasitic coupling and partial ground plane were used to accomplish wideband operations. The presented antenna has a wide bandwidth of 47% and a high efficiency of 95%, although its gain varies widely across the operational bandwidth. A coplanar waveguide fed circularly polarized antenna is presented in [5] for 60 GHz wireless communication. The proposed antenna is made comprised of an air cavity and a fused silica superstrate. A gold ring is put over the upper layer of fused silica to decrease surface wave losses. Patch employs diagonal slots to achieve left-hand circular polarisation. The depicted antenna has a bandwidth of more than 26% and an efficiency of 90%. The necessity for alignment precision is one of the structure's major constraints. Maintaining alignment precision in millimetre wave design is quite difficult. Jaiswal, Abegaonkar and Koul, 2019 [6] show a broadband patch antenna with recessed ground and an alumina ceramic substrate. Recessed ground allows for wideband activities and increased efficiency. When compared to conventional ground, the proposed antenna improves bandwidth by 9% and efficiency by 24.97%. In this design, complex manufacturing is a major challenge. Vettikalladi, Lafond and Himdi, 2009 [7] describe an aperture linked antenna based on a superstrate. The superstrate is half a wavelength above the aperture linked patch antenna. Over a wide bandwidth, a stable gain of more than 13 dB is obtained with 76% efficiency. The antenna's wide breadth and lack of alignment precision are significant drawbacks of this construction. Kim *et al.*, 2005 [8] illustrate a micro machined patch antenna consisting of a radiating patch supported by two metallic posts and a substrate with a feeding network and a coplanar ground plane. Dielectric losses are reduced since the patch is put in air. The illustrated antenna has an excellent bandwidth of 8.5 GHz, a high efficiency of 94%, and a gain of 9.9 dBi. This design has significant problems due to non-planar geometry, expensive manufacturing, and alignment precision. Haider, Alam and Sagor, 2018 [9] show a V-shaped patch antenna with a probe and a V-shaped metallic element as a radiating structure. When coplanar waveguide feeding is employed, a 0.787 mm thick Rogers RT /duroid 5880 dielectric substrate is used. Because of the thick substrate, a wide bandwidth and low radiation loss are obtained. With a radiation efficiency of 77.8%, a bandwidth of 8.6 GHz is obtained. Cross-polar components and an end-fire radiation pattern are provided by the thick substrate. Tiwari, Kumar and Bisht, 2011 [11] demonstrate a microstrip antenna atop a photonic band gap crystal made of periodic air gap dielectric. The discussed structure has a broad bandwidth and a high radiation efficiency. A bandwidth of 20.5% is reached, with

Article history: Received September 25, 2021; Accepted June 28, 2022

Tapan Nahar and Sanyog Rawat are with Department of Electronics and Communication Engineering, Manipal University Jaipur, India, *E-mail: sanyog.rawat@jaipur.manipal.edu

an efficiency of 76.74%. At 60 GHz, an omnidirectional radiation pattern with a directivity of 9.14 dB is produced. The primary constraint of this construction is its complex manufacturing. Abdulraheem *et al.*, 2014 [12] illustrate a reconfigurable circular patch antenna with a ring slot. To provide pattern reconfigurable features, two NMOS switches are utilised at various curvatures of the ring slot. At different switching locations, the proposed antenna delivers 5.7%, 3.3%, and 3.4% bandwidth with gains of 3.9 dB, 4.8 dB, and 4.5 dB, respectively. With the 70-degree shifting option in the radiation pattern, efficiency of more than 95% is attained. The antenna's limited bandwidth is a significant disadvantage. Xia *et al.*, 2020 [13] describe a metasurface antenna with coplanar waveguide feeding. A ring resonating structure with coplanar waveguide feeding is utilised, with a high dielectric constant glass substrate. To keep the material from oxidising, two polyamide substrates are utilised at the top and bottom. This antenna has an impedance bandwidth of 22.83% and a gain of 5.5 dB. It is difficult to obtain a low profile, planar, and cheap cost wideband highly efficient antenna with steady gain for V-band and W-band applications.

This article presents a planar gap coupled antenna with a tapered slotted ground. Among the many approaches mentioned, the gap coupled technique is utilised to attain wideband properties while remaining simple, planar, and easy to fabricate. Two closed-radius semi-circular patches are electromagnetically linked to provide multiple resonances and a wide bandwidth. To achieve consistent ultra wideband properties, a tapered slotted profile is employed. According to [11-16], a tapered slot antenna has unlimited bandwidth, a high gain, and a symmetrical radiation pattern. The bandwidth of an aperture antenna is determined by its length and breadth.

There are seven sections to this paper. Section I contains an introduction and a literature survey of antennas used for the W, V, and M bands. Section II explains the proposed design geometry. Section III illustrates the modelling results of the presented antenna. Section IV presents a quantitative analysis of the discussed antenna. Section V compares the performance of the developed antenna to that of previously reported antennas. Applications of discussed antenna are discussed in Section VI. Section VII consists of the conclusion.

II. ANTENNA DESIGN

Fig. 1 illustrates the proposed antenna geometry. It is made up of a semi-circularly driven patch that is excited by a 50 Ohm microstrip line. At the driven patch's linear edge, two notches are formed. A parasitic linked semi-circular patch is a driven patch. Tapered ground planes are utilised to achieve extremely wide bandwidth and stable radiation characteristics. Overlapping two-quarters of a circular-shaped metallic piece creates a tapered ground plane. The geometry of the ground plane is seen in Fig. 1. Table 1 shows the antenna's optimised design parameters. The substrate is Rogers RO 3006, which has a dielectric constant of 6.5, a loss tangent of 0.002, and a height of 0.402 mm. The radiator and ground layer are composed of copper layers with a thickness of 0.035 mm.

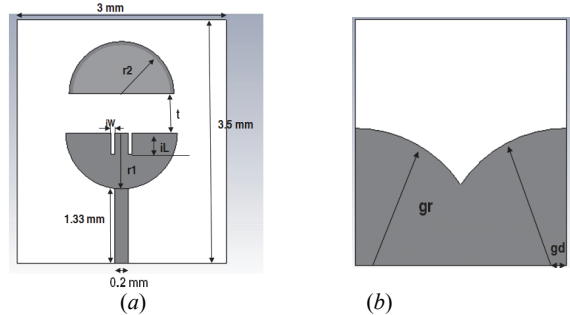


Fig. 1. Proposed antenna geometry: (a) front view and (b) back view

TABLE 1
DESIGN PARAMETERS OF ANTENNA

Radius of driven semi-circular patch (r1)	0.8 mm
Radius of parasitic semi-circular patch (r2)	0.75 mm
Gap between driven patch and parasitic patch (t)	0.57 mm
Radius of quarter circular metallic layers (gr)	1.8 mm
Displacement of centres of quarter circular metallic elements from corners (gd)	0.15 mm
Length of slot pairs at edges of semi-circular driven patch (iL)	0.6 mm
Width of slot pairs at edges of semi-circular driven patch iW	0.05 mm
Height of substrate (h)	0.42 mm
Length of substrate (L)	3.5 mm
Width of substrate (W)	3 mm
Width of 50 Ohm microstrip line	0.2 mm
Length of 50 Ohm microstrip line	1.33 m

III. SIMULATION RESULTS

Fig. 2 depicts the variations of the reflection coefficient (S_{11}) with frequency. It can be shown that the suggested antenna has an S_{11} of less than -10 dB from 57.5 GHz to 100 GHz and an impedance bandwidth of 70.83% at 60.4 GHz. The minimum reflection coefficients are around -60 dB, indicating that the feed and patch impedances are well matched.

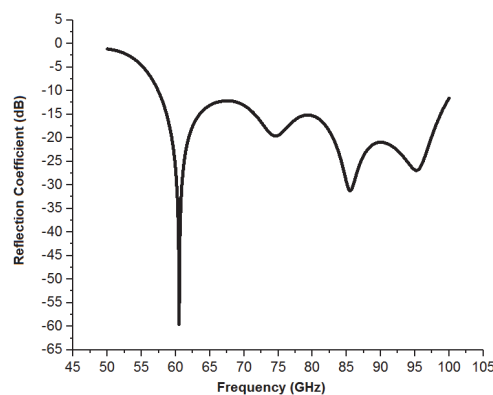


Fig. 2. Reflection coefficient (S_{11}) versus frequency plot

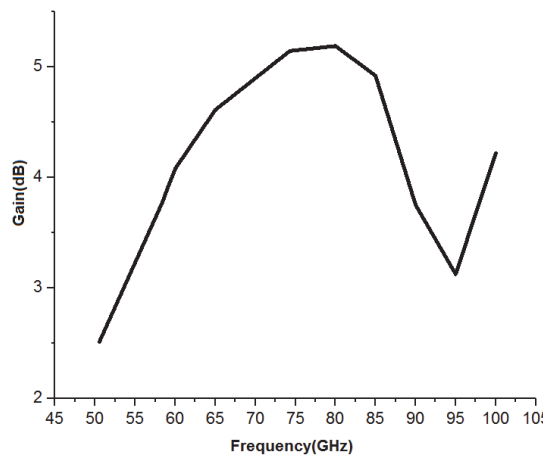


Fig. 3 Gain (dB) versus frequency plot

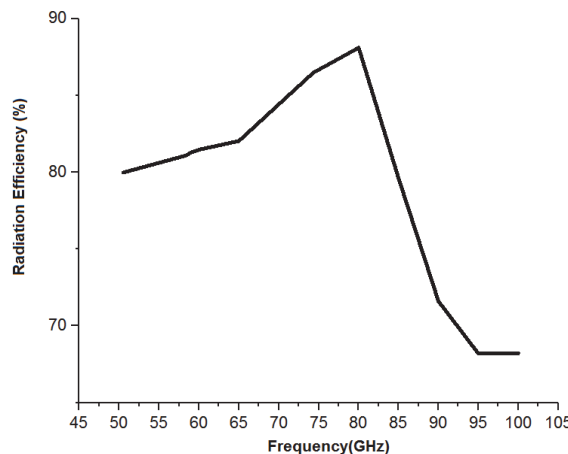


Fig. 4. Radiation efficiency versus frequency plot

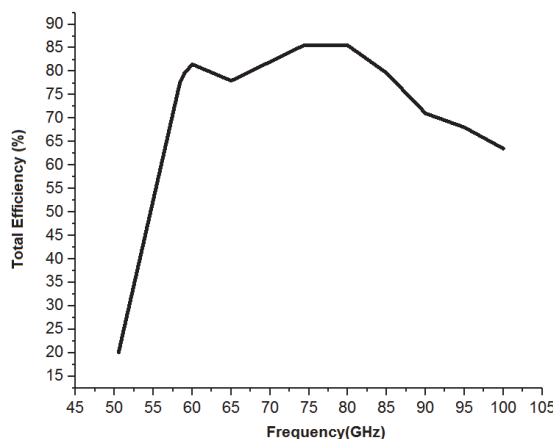


Fig. 5. Total efficiency versus frequency plot

Fig. 3 shows a gain versus frequency plot. It should be noted that the suggested antenna has a maximum gain of 5.187 dB at 80 GHz. Gain variations in the operational bandwidth are fewer than 3 dB.

Fig. 4 depicts a plot of radiation efficiency against frequency. It can be shown that that the highest radiation efficiency of 88.10% is reached at 80 GHz and that radiation efficiency is better than 68% across the whole operational bandwidth, indicating that the suggested antenna has the minimum radiation losses. Fig. 5 depicts a total efficiency vs frequency plot. At 80 GHz, the maximum efficiency is 85.5%, while total efficiency is more than 63% throughout all operating frequencies. At 60.4 GHz, both radiation efficiency and total efficiency are identical, indicating that there are no additional antenna losses.

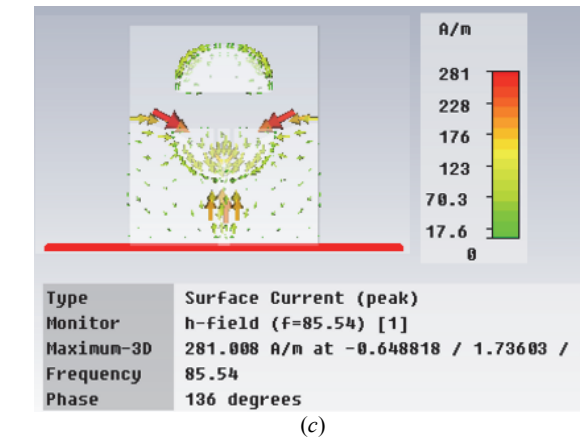
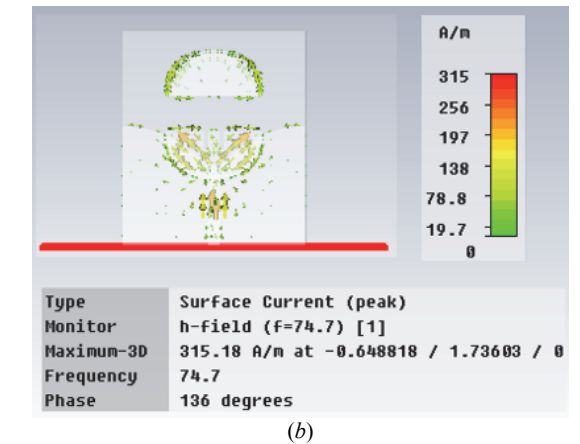
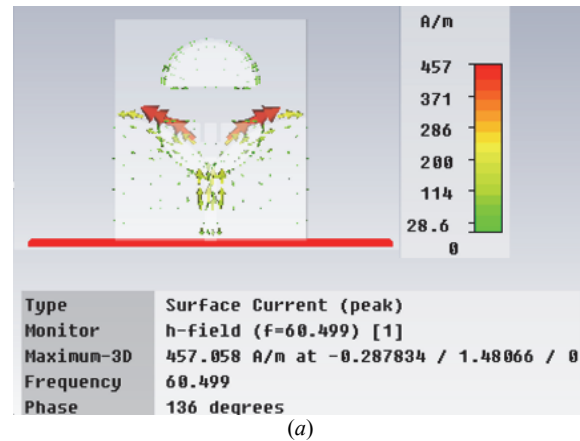


Fig. 6. Surface current distribution at: (a) 60.4 GHz, (b) 74.7 GHz, and (c) 85.5 GHz

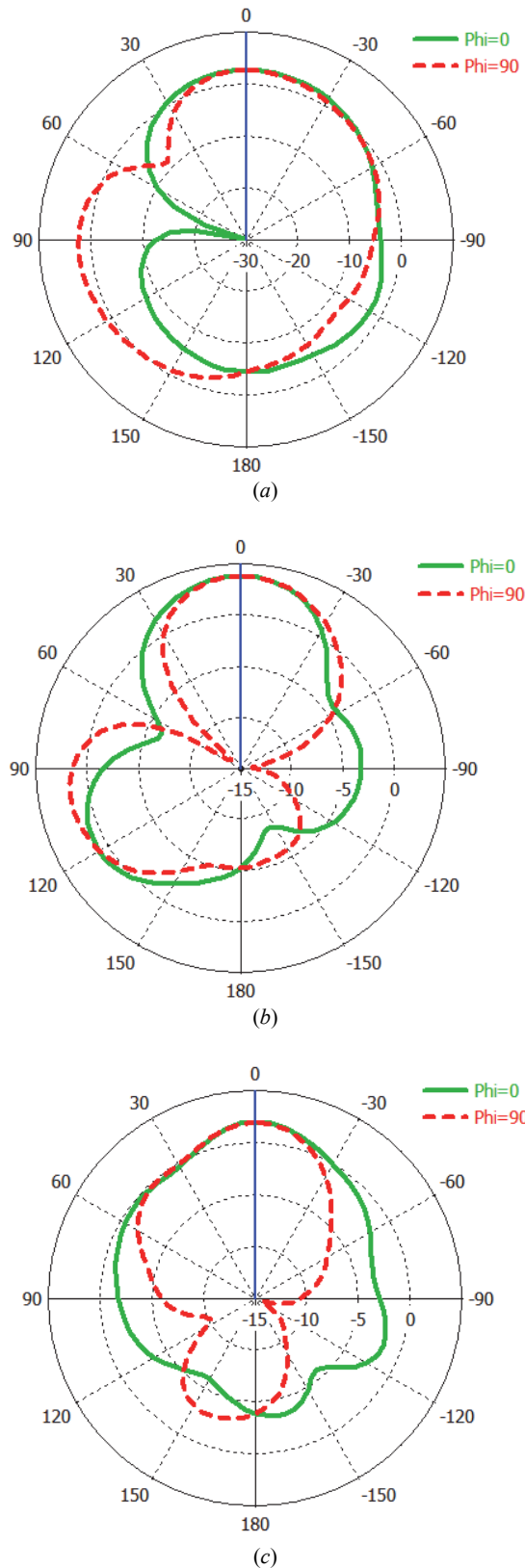


Fig. 7. Radiation pattern at: (a) 60.4 GHz, (b) 74.7 GHz, and (c) 85.5 GHz

Fig. 6 (a), (b), and (c) show the surface current distribution of an antenna at 60.4 GHz, 74.7 GHz, and 85.5 GHz, respectively. Maximum current is focused at patch edges and the tapering ground plane, as can be seen.

Fig. 7 (a), (b), and (c) show the radiation pattern of the proposed antenna at 60.4 GHz, 74.7 GHz, and 85.5 GHz, respectively. It should be observed that side lobe levels vary with frequency, although maximal radiation is nearly equal.

IV. ANALYSIS OF RESULTS

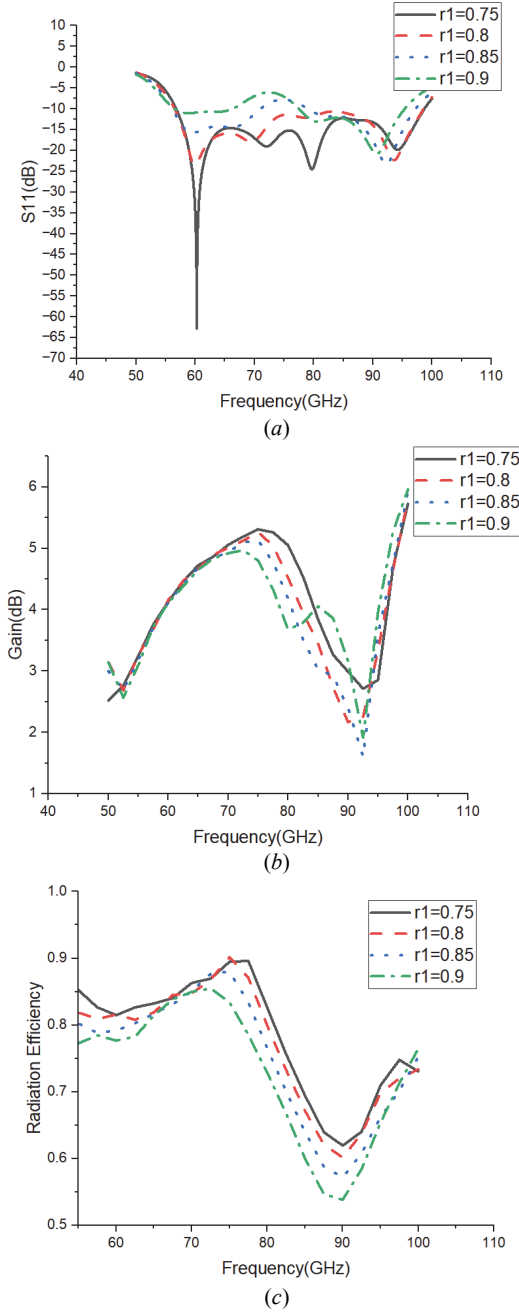


Fig. 8. Effect of driven patch radius (r_1) on: (a) reflection coefficient, (b) gain, and (c) radiation efficiency

Performance of proposed antenna is analysed by examining various geometrical parameters. Effect of driven patch radius on performance parameters reflection coefficient, gain and radiation efficiency is shown in Fig. 8 (a), (b) and (c) respectively. It may be noted from Fig. 8(a) that presented antenna provide minimum reflection coefficient at 60.4 GHz and wide bandwidth of 42.5 GHz for radius of 0.8 mm. When radius is increasing, the impedance matching performance between feed line and patch is reduced which can be verified from the increased values of S_{11} in plot. For larger radius values, gain and radiation efficiency are reduced due to increasing losses. Gain and radiation efficiency are both high at 0.8 mm radius.

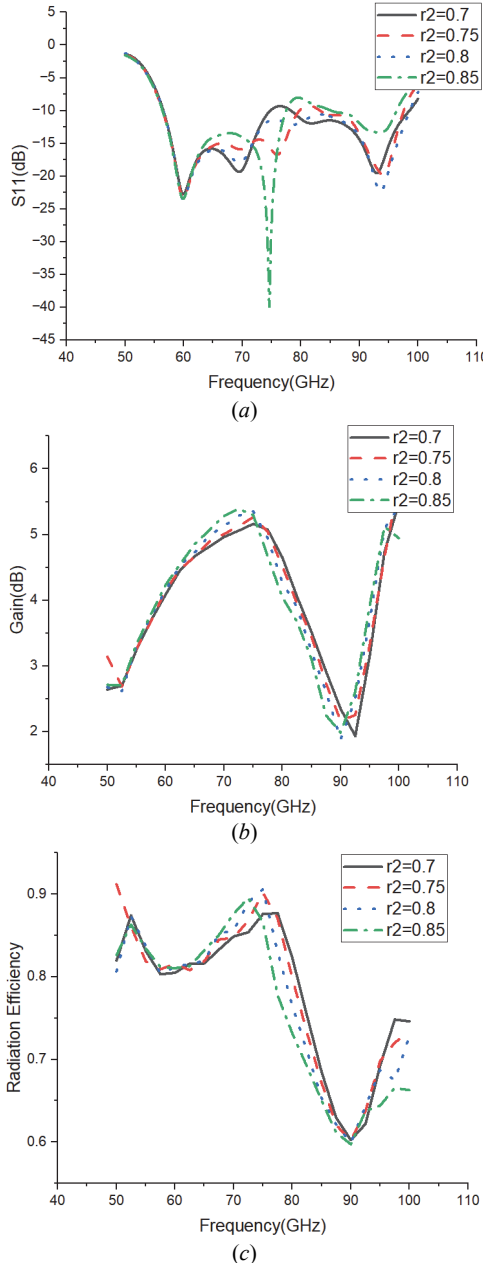


Fig. 9. Effect of parasitic patch radius (r_2) on: (a) reflection coefficient, (b) gain, and (c) radiation efficiency

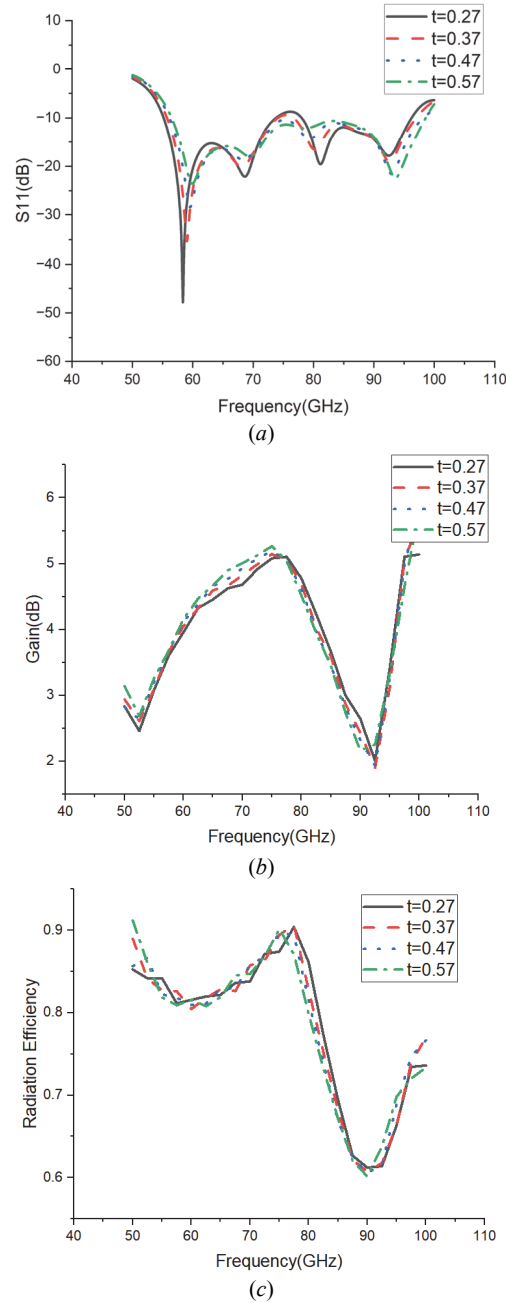


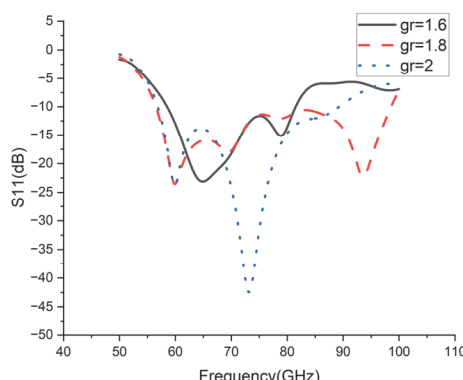
Fig. 10. Effect of spacing (t) between driven patch and parasitic patch on: (a) reflection coefficient, (b) gain, and (c) radiation efficiency

Fig. 9 (a), (b), and (c) show the reflection coefficient versus frequency plot, gain versus frequency plot, and radiation efficiency versus frequency plot for various values of r_2 . Because the radius of the driven patch is fixed, the initial resonance remains constant at 60.4 GHz. Because the radius of the parasitic patch is less than the radius of the driven patch, the second resonant frequency is greater than the first resonant frequency. The second resonant frequency decreases as the radius increases, and the return loss increases as the coupling reason of the fringing field between the parasitic

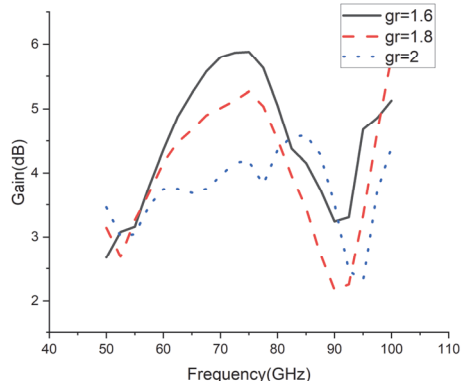
patch and the driven patch changes. As radius is increasing, radiating aperture is increasing so gain and efficiency are increasing.

Fig. 10 depicts the effect of distance between the driven patch and the parasitic patch on the performance parameter.

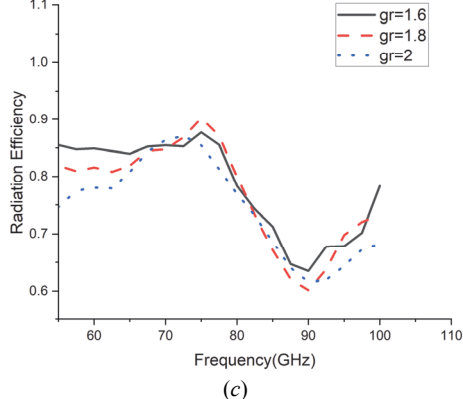
As the spacing grows, the return loss decreases and the impedance effectively matches at all frequencies. The gain of an antenna increases with increasing spacing at lower frequencies because the radiating area increases, while at higher frequencies this feature is inverted because field coupling is reduced. The radiation efficiency is about the same.



(a)



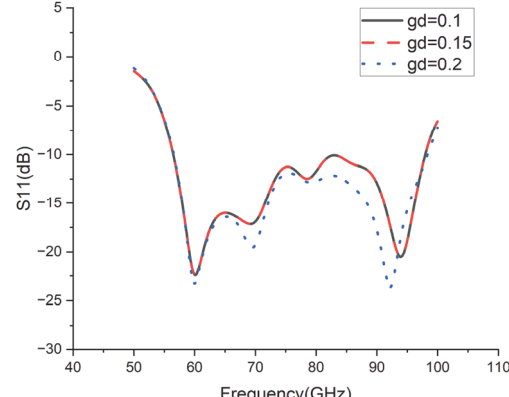
(b)



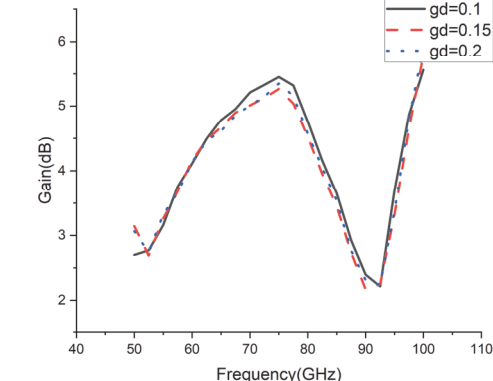
(c)

Fig. 11. Effect of on radius(gr) of quarter circles in the ground:
(a) reflection coefficient, (b) gain, and (c) radiation efficiency

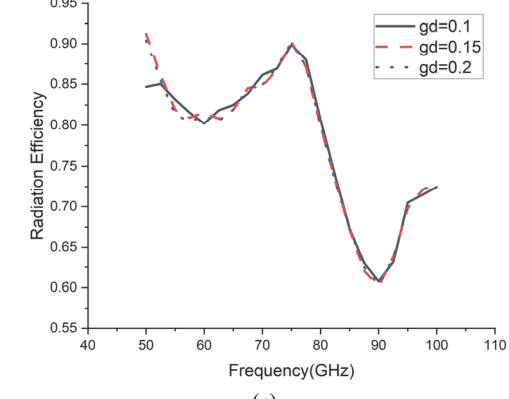
Fig. 11 depicts the effect of the radius of quarter circles in the ground on radiation performance. As the radius changes, the slot width decreases and the curvature of tapered slots changes. Matching performance degrades as the radius increases. With wideband characteristics, excellent impedance matching is attained at a radius of 1.8 mm. Fig. 10(a) depicts a plot of the reflection coefficient against frequency. At 60.4 GHz and 85.4 GHz, return loss is 60 dB and 30 dB, respectively. Radiation efficiency and gain are optimised at 1.5 mm radius, as illustrated in Fig. 11 (c) and (b). High gain may be attained by using a tapered slot antenna with a big opening aperture [15].



(a)



(b)



(c)

Fig. 12. Effect of displacement of centers of the quarter circles from the corner (gd) in ground on: (a) reflection coefficient, (b) gain, and (c) radiation efficiency

The displacement of the quarter circle centres from the corner in the ground is defined as parameter gd . The flaring width of the tapered slot in the ground decreases as gd increases. Flaring width is optimised at 0.15 mm displacement. When the flare width decreases, the impedance matching performance, gain, and efficiency all decrease. The effect of displacement of the centres of the quarter circles from the corner in the ground on the reflection coefficient, gain, and radiation efficiency is shown in Fig. 12.

TABLE 2
PERFORMANCE COMPARISON OF PROPOSED ANTENNA WITH
REPORTED 60 GHZ ANTENNAS

Work	Size [mm ³]	Impedance bandwidth [%]	Antenna type	Efficiency [%]	Peak gain [dBi]
This work	3*3.5*0.4	70.83	Microstrip antenna	85.3	5.23
[4]	3*3.5*0.4	47	Microstrip antenna	95	3
[5]	4.849*5.555*1.4	26	Circularly polarized	90	7
[6]	2.269*3.132*0.4	11.33	Patch antenna with recessed ground	87.44	6.94
[7]	5.5*5.5*3.58	6.8	Superstrate antenna	76	14.6
[8]	6.2*4.2*0.2	14.5	CPW fed post supported patch antenna	94%	9.9
[9]	5*2.75*0.787	14.3	V shaped 3D dipole	77.8	5.45
[10]	5.6*5.6*0.762	4.76	Charge slot antennas with diffused engineered line	-	5.48
[11]	2.5*1.5*0.4	20.53	Photonic band gap antenna	75.53	7.9
[12]	5.4*5.4*0.504	5.7	Circular dish microstrip antenna with ring slot	95	3.9
[13]	1.5*1.5*0.3	22.83	Metasurface antenna	-	5.5

V. PERFORMANCE COMPARISONS WITH REPORTED ANTENNAS

Table 2 compares the performance of the proposed antenna to that of previously reported 60 GHz antennas. It should be noticed that the impedance bandwidth of the pr

antenna is greater than that of the stated antennas. The presented antenna is smaller than the reported antennas [5], [7–10], and [12]. Gain and efficiency of antenna is comparable to some structures and higher than some structures. The presented antenna features a low profile, single layer, and compact design with an extremely wide bandwidth.

VI. APPLICATION AREAS OF PROPOSED ANTENNA

IEEE defines the V-band as a frequency range of 40 to 75 GHz. The IEEE employs letters to denote a frequency range of 1 to 110 GHz [2]. In many countries, the V-Band is free of charge, and it is most commonly used for wireless backhaul and point-to-point/point-to-multipoint radio connections. These systems are typically utilised for line-of-sight communications with large capacity. This band was used in the point-to-point radio solution market due to the availability of a larger bandwidth. Radio connections operating in the V band may be densely deployed in congested cities without causing interference, and without the need for costly, sluggish, and disruptive cable and fibre optic installation. Today, radios with full-duplex data speeds of up to 10 Gbps across distances of up to one mile are readily accessible. IEEE launched 802.11ad wireless access technologies (also known as WiGig) in the V band in 2013, allowing devices to communicate wirelessly at multi-Gigabit rates and provide high-definition video over shorter distances. The Federal Communications Commission in the United States has designated the frequency range 57 to 71 GHz for unlicensed wireless networks [4]. For a long time, the V band, which spans 57 to 66 GHz, has been utilised for high-capacity terrestrial millimetre wave communications systems. The significant absorption of signals due to oxygen at this frequency is one difficulty that occurs while using the V-Band. As a result of the high signal absorptions, the V-Band typically has a range of about 2 kilometres [2–3].

The IEEE defines the W-band as a frequency range of 75 to 110 GHz. The IEEE uses letters to denote a frequency range of 1 to 170 GHz [2]. The W band overlaps with the M band, which is defined by NATO (60 to 100 GHz). Automotive radars, satellite communication, astronomy, defence, and security applications are just a few of the applications that employ this spectrum. The International Telecommunication Union has allocated the bands 71 to 76 GHz and 81 to 86 GHz for satellite services. Automotive radars also use the 77 GHz frequency window. Radar targets and millimeter-wave radar search, both for civilian and military reasons, satellite communications (SATCOM), different military and civilian tracking applications, and so on are currently recognised application fields [1–3]. Naturally, non-destructive testing (NDT) and security-screening procedures for inspecting diverse materials and detecting/visualizing internal flaws/abnormalities, as well as for concealed objects, are major applications. There are also a variety of passive millimeter-wave screening devices (i.e., those that function without the use of radiation) that are utilised for the detection of weapons and illegal goods that operate at frequencies about 94 GHz [2–3]. A frequent choice for different radars used in automated cruise control systems is the frequency of 77 GHz (and their

respective radars). The frequency of 94 GHz is regarded as the "atmospheric transparency window", whereas millimeter-waves and THz radiation are known to be extensively absorbed at higher frequencies. These characteristics make imaging millimeter-wave radar possible and attract a variety of applications in military, astronomy, and security, among others. Another significant characteristic that attracts many communication technologies that now have to 'tame' free space and function at very high altitudes is W band's impressive data rate throughput capacity. For satellite services, the ITU (International Telecommunication Union), the major regulatory body in this field, has assigned frequency segments of (81–86) GHz and (71–76) GHz. All major commercial satellite operators are showing increased interest in W band slots for satellite communication, indicating that they are preparing to launch commercial projects in W band in the not-too-distant future [1-3]. Microwave W band has been used in mobile communication backhaul infrastructure for almost two decades, and about half of the world's mobile web sites currently use connections via radio networks based on Millimeter and Microwave waves. Furthermore, we are witnessing the evolution of 4G into the 5G communication age, with experts universally agreeing that W band can completely fulfil 5G demands and needs, both in terms of data transport and network [3]. TeraSense imaging technology, which predominantly uses the W band spectrum, allows for rapid non-destructive assessment of flaws in uniform materials and coated surfaces, as well as the detection of concealed objects (around 100 GHz). Statistics show that security screening applications (homeland security) and non-destructive testing (NDT) are the most popular [1-3].

VII. CONCLUSION

This communication proposes a wideband electromagnetically coupled patch antenna with tapered slotted ground for W and V band applications. By combining a tapered slot structure with parasitically coupled patches, a wide bandwidth is obtained. The proposed antenna resonates from 58.4 GHz to 100 GHz and has a radiation efficiency of 88.10%. Gain is nearly constant throughout a wide bandwidth, varying by less than 1 dB. It can be readily integrated with RF integrated circuits and system on chip because of its low profile, planar, compact, and simple construction. The presented antenna, with its wideband operation, steady gain, and moderate efficiency, can be used in a variety of applications, including industrial automation, tera-hertz imaging, security applications, defense applications, automotive radars, wireless personal area networks, wireless backhaul, satellite communication, point-to-point/point-to-multipoint radio connections, astronomy, defense and many more.

REFERENCES

- [1] E. Cianca, T. Rossi, A. Yahalom, Y. Pinhasi, J. Farserotu and C. Sacchi, "EHF for Satellite Communications: The New Broadband Frontier", *Proceedings of the IEEE*, vol. 99, no. 11, pp. 1858-1881, Nov. 2011, doi: 10.1109/JPROC.2011.2158765
- [2] "IEEE Standard Letter Designations for Radar-Frequency Bands", in IEEE Std 521-2002 (Revision of IEEE Std 521-1984), pp. 1-10, 8 Jan. 2003, doi: 10.1109/IEEESTD.2003.94224.
- [3] B.A. Shelters, "Technical Report on Satellite Communications in the V and W Band: Tropospheric Effects", *Air Force Institute of Technology Wright-Patterson AFB OH*, 2018-03-22, <https://apps.dtic.mil/sti/citations/AD1056212>.
- [4] S. Singhal, "Compact Wideband Antenna for 60 GHz Millimeter Wave Applications", *Microwave Review*, vol. 27, no. 1, July 2021, pp. 23-27.
- [5] R. Zhou, D. Liu and H. Xin, "Design of Circularly Polarized Antenna for 60 GHz Wireless Communications", *2009 3rd European Conference on Antennas and Propagation*, Berlin, 23-27 March 2009, pp. 3787-3789.
- [6] A. Jaiswal, M.P. Abegaonkar and S.K. Koul, "Highly Efficient, Wideband Microstrip Patch Antenna with Recessed Ground at 60 GHz", *IEEE Transactions on Antennas and Propagation*, vol. 67, no. 4, pp. 2280-2288, April 2019, doi: 10.1109/TAP.2019.2894319.
- [7] H. Vettikalladi, O. Lafond and M. Himdi, "High-Efficient and High-Gain Superstrate Antenna for 60-GHz Indoor Communication", *IEEE Antennas and Wireless Propagation Letters*, vol. 8, pp. 1422-1425, 2009, doi: 10.1109/LAWP.2010.2040570.
- [8] J.-G. Kim, H.S. Lee, H.-S. Lee, J.-B. Yoon and S. Hong, "60-GHz CPW-Fed Post-Supported Patch Antenna using Micromachining Technology", *IEEE Microwave and Wireless Components Letters*, vol. 15, no. 10, pp. 635-637, October 2005, doi: 10.1109/LMWC.2005.856690.
- [9] M.F. Haider, S. Alam and M.H. Sagor, "V-Shaped Patch Antenna for 60 GHz mm Wave Communications", *2018 3rd International Conference for Convergence in Technology (I2CT)*, Pune, India, pp. 1-4, 06-08 April 2018, doi: 10.1109/I2CT.2018.8529809.
- [10] P.M. Paul, K. Kandasamy, S.S. Mohammad and B.M., "Diffusion Engineered Emission Line Charged Slot Antenna of an UWB Execution", *IEEE Antennas as Well as Wireless Transmission Letters*, vol. 18, pp. 323-327, December 2018.
- [11] R.N. Tiwari, P. Kumar and N. Bisht, "Rectangular Microstrip Patch Antenna with Photonic Band Gap Crystal for 60 GHz Communications", *PIERS Proceedings*, Suzhou, China, September 12-16, 2011, pp. 856-859.
- [12] Y.I. Abdulraheem, A.S. Abdullah, H.J. Mohammed, B. Mohammed and R.A. Abd-Alhameed, "Design of Radiation Pattern-Reconfigurable 60-GHz Antenna for 5G Applications", *Journal of Telecommunications*, vol. 27, no. 2, pp. 7-11, October 2014.
- [13] H.-Y. Xia, J.-C. Hu, T. Zhang, L.-M. Li and F.-C. Zheng, "Integrated 60-GHz Miniaturized Wideband Metasurface Antenna in a GIPD Process", *Frontiers of Information Technology & Electronic Engineering*, vol. 21, pp. 174-181, 2020, doi: 10.1631/FITEE.1900453
- [14] R. Singha and V. Damera, "Artificial Material Integrated Ultra-Wideband Tapered Slot Antenna for Gain Enhancement with Band Notch Characteristics", *Radioengineering*, vol. 27, no. 1, pp. 54-62, April 2018.
- [15] R.G. Anu and S.S. Kumar, "Radiating Flare Design of Tapered Slot Loaded Vivaldi Antenna Using Fourier Series Approach", *International Journal of Engineering and Advanced Technology (IJEAT)*, vol. 5, no. 3, pp. 39-43, February 2016.
- [16] E. de Lera Acedo, E. Garcia, V. González-Posadas, J.L. Vazquez-Roy, R. Maaskant, and D. Segovia, "Study and Design of a Differentially-Fed Tapered Slot Antenna Array", *IEEE Transactions on Antennas and Propagation*, vol. 58, no. 1, pp. 68-78, January 2010, doi: 10.1109/TAP.2009.2036193.

- [17] I.K. Ukaegbu and K. A.A. Gamage, "Parametric Analysis and Bandwidth Optimisation of Hybrid Linear-exponential Tapered Slot Vivaldi Antennas", *Loughborough Antennas & Propagation Conference (LAPC 2017)*, 2017, pp. 1-5, doi: 10.1049/cp.2017.0279.
- [18] N.O. Parchin, M. Shen, and G.F. Pedersen, "Small-Size Tapered Slot Antenna (TSA) Design for use in 5G Phased Array Applications", *Applied Computational Electromagnetics Society Journal*, vol. 32, no. 3, pp. 193-202, March 2017.
- [19] M.M. Mohanna, E.A. Abdallah, H. El-Hennawy, and M.A. Attia, "A Novel High Directive Willis-Sinha Tapered Slot Antenna for GPR Application in Detecting Landmine", *Progress In Electromagnetics Research C*, vol. 80, pp. 181-198, 2018, doi: 10.2528/PIERC17111904.
- [20] T. Nahar and S. Rawat, "Survey of Various Bandwidth Enhancement Techniques used for 5G Antennas", *International Journal of Microwave and Wireless Technologies*, vol. 14, no. 2, pp. 204-224, March 2022, doi: 10.1017/S1759078720001804.